

Pyrolysis-Tuned Dielectric-Conductive Transition in Banana Peel-Derived Biochar for Organic Electronics

Divya Naina, Er. Naseer Ahmad
Punjab Technical University, India

Abstract - This study conducts a systematic examination of biochar derived from banana peels as a sustainable functional material that demonstrates a controllable dielectric-to-conductive transition through pyrolysis engineering. Biochar samples produced at temperatures ranging from 300 to 600 °C exhibit substantial structural transformation from oxygen-rich amorphous carbon to graphitised sp^2 domains. Dielectric spectroscopy shows that the permittivity can be changed ($k \approx 3-12$), and electrical measurements show that the material goes from being an insulator to a conductor based on percolation thresholds. Biochar-polymer composite thin-film devices have low leakage current (about 10^{-7} A) and stable capacitance behaviour. The transition process arises due to gradual carbonisation, reduction of functional groups, and formation of pathways for conductivity. These findings indicate that biochar derived from banana peels can serve as a promising alternative material for future generation flexible/organic electronics as it is inexpensive and environmentally friendly.

Index Terms - Biochar, Dielectric materials, Organic electronics, Sustainable electronics, OFET, Pyrolysis

1. INTRODUCTION

The rapid development of organic and flexible electronics creates a necessity for lightweight, inexpensive, and sustainable materials. The dielectric layer plays an important role since it determines the capacity for charge storage, leakage current, and stability of the device.

SiO_2 and Al_2O_3 are typical dielectrics that operate effectively; however, they are costly, rigid, and unsustainable in their fabrication processes. Therefore, increasing interest emerges in bio-derived materials as potential candidates.

Biochar produced through the pyrolysis of biomass presents unique advantages, including tunability in electrical performance, a highly porous structure, and environmental sustainability. Banana peels are abundant in agriculture as organic waste rich in carbon-based substances and mineral

impurities. These qualities make banana peels a promising feedstock for functional materials.

This study explores the controllable tuning of the electrical features of biochar obtained from banana peels and demonstrates the usage of biochar as a dielectric layer in organic electronics. To the best of the authors' knowledge, no prior works have revealed tunable dielectric-conductor transitions of banana peel-derived biochar at the device level. This study bridges the gap between sustainable material production and functional application in organic electronics.

2. EXPERIMENTAL METHODOLOGY

A schematic illustration of the overall fabrication process is shown in Fig. 1.

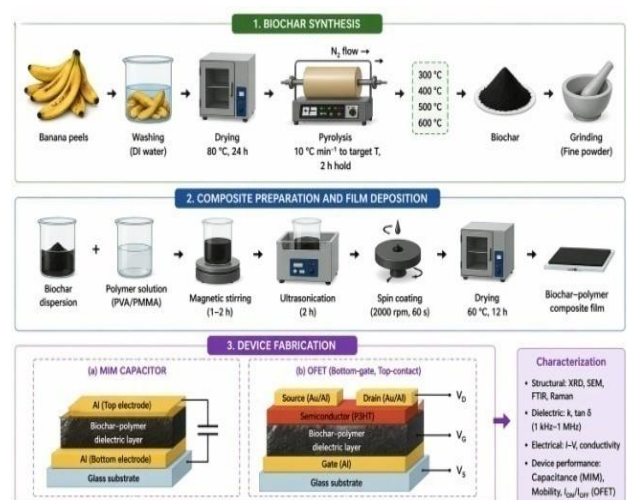


Fig. 1. Schematic illustration of biochar synthesis, composite preparation, and device fabrication.

Fig. 1. Schematic illustration of banana peel-derived biochar synthesis, composite film preparation, and fabrication of MIM capacitor and OFET devices.

2.1 Biochar Synthesis

Banana peels were first washed using deionized water to clean them from any impurity on the surface. The washed material was then dried at 80 °C for 24 hours before cutting it into small pieces. Pyrolysis process was performed in a tubular furnace under the flow of nitrogen gas (with purity level of 99.99%) to have inert atmosphere.

Heating rates were set to 10 °C/min in order to achieve different temperatures of 300, 400, 500 and 600 °C, which would be held for two hours. The process of pyrolysis was performed under nitrogen atmosphere, which was later turned off after cooling down to room temperature. The resulting biochar sample was crushed using agate mortar to make fine powder.

2.2 Preparation of Biochar–Polymer Composite Films

The biochar powder was added separately into PVA and PMMA matrices to produce composite dielectric films.

In the case of PVA-based films, the PVA was dissolved in distilled water at 80 °C with constant stirring, and then biochar (5–10 wt%) was added. In the case of PMMA-based films, the PMMA was dissolved in acetone, and then biochar was mixed with it under magnetic stirring.

The resultant mixture was sonicated for 2 hours to homogeneously disperse the biochar and prevent particle agglomeration. The films were prepared by spin-coating process at 2000 rpm for 60 seconds, and then dried at 60 °C for 12 hours.

2.3 Structural and Chemical Characterization

X-ray Diffraction (XRD): Carried out with Cu-K α radiation ($\lambda = 1.5406 \text{ \AA}$) for the 2θ range between 10° and 80° to assess crystalline characteristics and structure transformation.

Scanning Electron Microscopy (SEM): Done with accelerating voltage ranging from 10 to 15 kV to determine surface features, porosity and dispersion of biochar within the polymer.

Fourier Transform Infrared Spectroscopy (FTIR): Measured in the range of 400–4000 cm^{-1} to characterize functional group and chemical bond modification during thermal pyrolysis.

Raman Spectroscopy: Done to determine graphitic structures through D-bands ($\sim 1350 \text{ cm}^{-1}$) and G-bands ($\sim 1580 \text{ cm}^{-1}$) analysis.

2.4 Electrical and Dielectric Measurements

The dielectric parameters such as dielectric constant (k) and loss tangent ($\tan \delta$) were determined through a precise LCR meter operating at a frequency range from 1 kHz to 1 MHz.

In determining the electrical behavior of the material, current-voltage (I-V) characteristics were performed by a source-measure unit at ambient temperature. Electrical conductivity was determined based on resistance and geometrical dimensions.

2.5 Device Fabrication and Testing

(a) MIM Capacitors

Metal–Insulator–Metal (MIM) capacitors were fabricated using a sandwich structure. Aluminum (Al) bottom electrodes were deposited on glass substrates via thermal evaporation. The biochar–polymer composite layer was spin-coated as the dielectric layer, followed by deposition of top Al electrodes using a shadow mask to define the active device area.

Capacitance–frequency characteristics and leakage current behavior were measured to evaluate dielectric performance.

(b) OFET Fabrication

OFET devices were fabricated with the bottom-gate and top-contact structure. The biochar composite material was used for the gate dielectric layer, and P3HT was used as the active layer.

The source and drain contacts (Au/Al) were deposited by thermal evaporation. The device performances were characterized based on the charge mobility, threshold voltage, and on-off current ratio. The device structures of MIM capacitor and OFET are illustrated in Fig. 2.

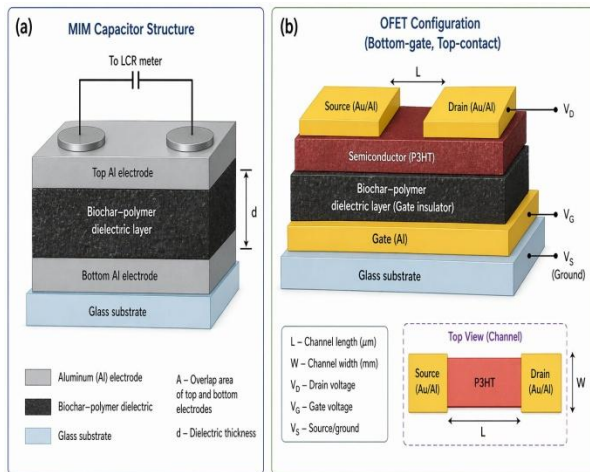


Fig. 2. Device architectures: (a) MIM capacitor, (b) OFET configuration.

3. RESULTS AND DISCUSSION

3.1 Structural Evolution of Biochar

The structural transformation of banana peel-derived biochar with increasing pyrolysis temperature was analyzed using X-ray diffraction (XRD) and Raman spectroscopy, as shown in Fig. 3. The intensity ratio (I_D/I_G) decreases with increasing temperature, indicating improved graphitic ordering and reduced structural defects.

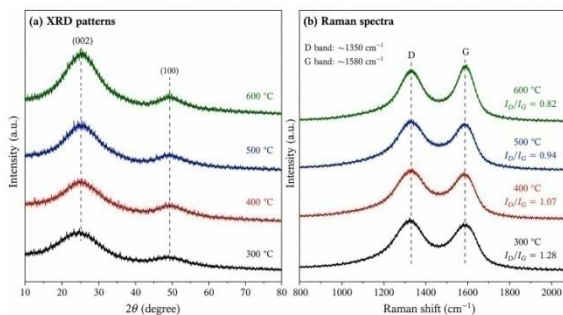


Fig. 3. Structural characterization of banana peel-derived biochar at different pyrolysis temperatures. (a) XRD patterns showing broad (002) peak around 24–26° and (100) peak around 43–45°, indicating turbostratic carbon structure. (b) Raman spectra exhibiting D band (~1350 cm^{-1}) and G band (~1580 cm^{-1}). The decrease in I_D/I_G ratio with increasing temperature confirms improvement in graphitic ordering and reduction of structural defects.

Under low temperatures (300–400 °C), XRD shows that the diffraction peaks are broad, meaning that amorphous carbon dominates. The appearance of a broad peak at (002) at around ~24° when the temperature rises from 500 °C to 600 °C implies the creation of turbostratic graphitic regions.

The Raman analysis further confirms this with the detection of a D band (~1350 cm^{-1}) and a G band (~1580 cm^{-1}). This gradual transformation is essential for influencing the electrical and dielectric characteristics of the carbon material.

3.2 Electrical Conductivity and Percolation Transition

The electrical conductivity of biochar exhibits a strong dependence on pyrolysis temperature, as shown in Fig. 4.

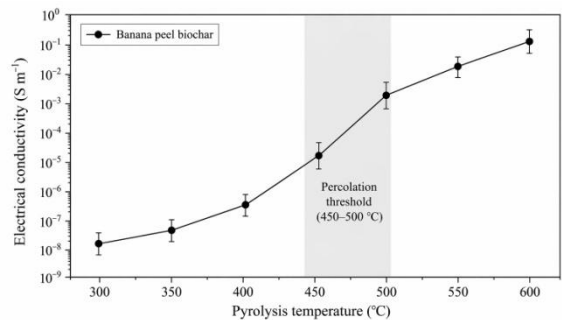


Fig. 4. Electrical conductivity of banana peel-derived biochar as a function of pyrolysis temperature. The shaded region represents the percolation threshold where interconnected conductive networks are formed.

The conductivity at 300 °C is very small (~ 10^{-8} S/m) because of insulating nature caused by oxygen-containing functional groups without any conduction path. With increasing temperature, conductivity increases slowly but sharply after 450 °C, attaining a value of ~ 10^{-1} S/m at 600 °C.

Percolation threshold is evident from 450–500 °C due to the formation of clusters which get connected to give rise to conduction paths.

This is a result of elimination of functional groups like hydroxyl group (-OH), carboxyl group (-COOH), formation of sp^2 carbon network, and charge carrier path formation.

Hopping mechanism of charge transport occurs at the intermediate temperature, whereas above that temperature percolation mechanism occurs.

3.3 Dielectric Properties

The dielectric behavior of the biochar-polymer composite films is shown in Fig. 5.

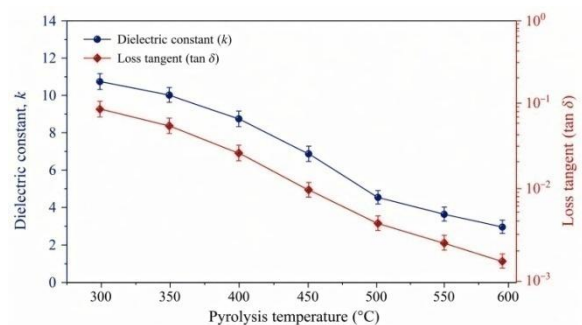


Fig. 5. Variation of dielectric constant (k) and loss tangent ($\tan \delta$) of biochar-polymer composite films with pyrolysis temperature (measured at 10 kHz).

During the process of pyrolysis when temperatures are low, the value of k (dielectric constant) is very high (10-12). This is mainly due to the dipole polarization, which arises on account of oxygen containing functional groups. But when the temperatures increase, the value of k decreases to about 3 at 600°C.

The $\tan \delta$ also falls with an increase in temperature, suggesting that there is an improvement in dielectric performance and less energy loss. It is evident that dielectric stability is maintained across a broad spectrum of frequencies (1kHz to 1MHz), making the material suitable for use in capacitors and gate dielectrics. All the dielectric properties were measured at 10 kHz except where noted otherwise.

3.4 MIM Capacitor Performance

The performance of MIM capacitors fabricated using biochar composite films is presented in Fig. 6.

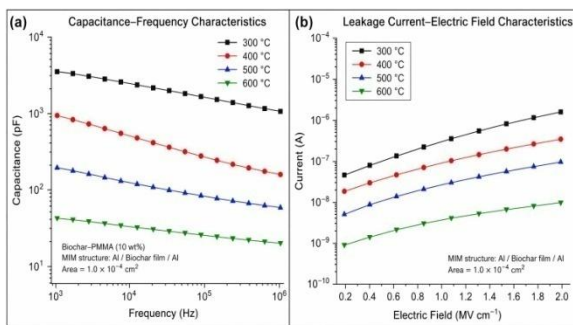


Fig. 6. MIM capacitor performance of biochar-based dielectric films: (a) capacitance–frequency characteristics and (b) leakage current as a function of applied electric field. Capacitance slightly decreases with frequency, while leakage current remains low ($\sim 10^{-7}$ – 10^{-8} A), indicating good insulating behavior.

Fig. 6. MIM capacitor performance: (a) capacitance–frequency characteristics and (b) leakage current as a function of applied electric field for biochar-based dielectric films.

Capacitance shows a decrease with increasing pyrolysis temperature, which is expected based on the reduced dielectric constant. Nevertheless, the capacitors show consistent capacitance values within the tested frequencies. In leakage current measurements (Fig. 6b), the current values are very low (approximately 10^{-7} to 10^{-8} A), thus confirming a good insulator nature, particularly for biochars obtained at lower temperatures. Moreover, breakdown voltage shows an increase with an increase in temperature, demonstrating that biochars obtained at higher carbonization temperatures have better structural properties with reduced defect concentration. These findings clearly show that biochar thin films

fabricated at moderate temperatures (400–500 °C) possess suitable dielectric characteristics.

3.5 OFET Device Characteristics

The transfer characteristics of OFET devices fabricated using biochar-based dielectric layers are shown in Fig. 7.

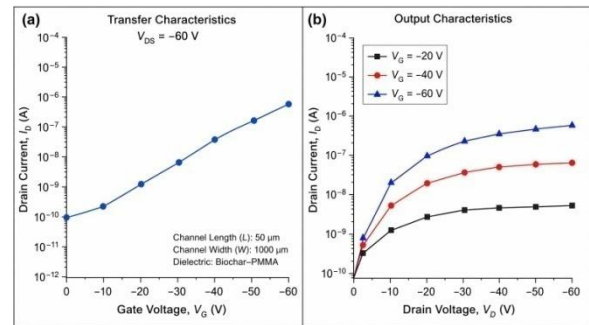


Fig. 7. OFET characteristics: (a) transfer characteristics ($V_{DS} = -60$ V) and (b) output characteristics at different gate voltages, demonstrating improved charge transport behavior with increasing pyrolysis temperature.

The field-effect mobility shows an enhancement from 10^{-3} to 10^{-2} $\text{cm}^2/\text{V}\cdot\text{s}$ due to increased pyrolysis temperatures since there are better interface characteristics, fewer trap states, and improved transport properties of charge carriers.

There is also a shift towards negative threshold voltages indicating an improvement in the injection characteristics of the charge carriers due to fewer traps.

The ratio of on/off currents increases greatly (from 10^3 to 10^5), which shows proper switching behavior. Such results show good integration capability of biochar dielectrics with organic semiconductors like P3HT.

3.6 Dielectric–Conductive Transition Mechanism

The transition from the dielectric to the conducting state depends on the structural and chemical changes produced as a result of pyrolysis. At lower temperatures, the dominant species are insulating functional groups; hence, the system is characterized by dipole moments. In intermediate temperatures, there are sp^2 clusters which facilitate hopping conduction of charge carriers. With further increase in temperature, there is formation of a conductive network that leads to charge transport through percolation. The transition could alternatively be understood as a consequence of reduced bandgap and delocalization of carriers.

These results are in line with previous observations made on carbon materials synthesized from biomasses where charge transport increases with pyrolysis temperature. Any slight

variations in measured parameters could be attributed to heterogeneity in biomass samples and processes involved.

4. SUSTAINABILITY AND IMPACT

The suggested approach presupposes the employment of agricultural waste, thus promoting resource management and their recycling. What is more important, the approach helps mitigate the environmental footprint owing to decreased reliance on regular non-biodegradable material. Another point is that it is due to the application of biochar that it would be possible to develop inexpensive electronic goods. Therefore, the presented technology can be regarded as an embodiment of the circular economy model. The low-temperature treatment and recycling of organic waste have a lower carbon footprint in comparison with standard inorganic dielectrics.

5. LIMITATIONS OF THE STUDY

But there are a few limitations that should be considered. To begin with, the absence of large-scale experiments that can prove the repeatability and scalability of the phenomenon can be viewed as one such limitation. Secondly, the issue concerns the lack of information regarding the homogeneity of the film of the biochar-polymer composite that can influence the performance of the device.

6. CONCLUSION

This study has shown that biochar created from the skins of bananas is viable and modifiable dielectric material for organic electronics. The process of pyrolysis enables controlled tuning of electrical properties through the manipulation of changing electrical insulation into conductivity. This implies that biochar can be used as eco-friendly replacement for current dielectric materials in flexible electronics.

The tunability and applicability of biochar make it a good candidate for green electronics on a grand scale. This study demonstrates, for the first time, a tunable dielectric–conductive transition in banana peel-derived biochar with device-level validation.

7. REFERENCES

- [1] C. Das, S. Tamrakar, A. Kiziltas, X. Xie, Incorporation of biochar to improve mechanical, thermal and electrical properties of polymer composites, *Polymers* 13 (2021) 2663. <https://doi.org/10.3390/polym13162663>
- [2] N.T.M. Tam, Y. Liu, H. Bashir, et al., Synthesis of porous biochar containing graphitic carbon derived from lignin biomass, *Front.*

- Chem.* 8 (2020) 274. <https://doi.org/10.3389/fchem.2020.00274>
- [3] K. Wang, X. Gong, X. Ye, et al., Dielectric engineering of biochar for microwave absorption, *Carbon* 228 (2024) 119326. <https://doi.org/10.1016/j.carbon.2024.119326>
- [4] Biochar for electrochemical applications, *Curr. Opin. Green Sustain. Chem.* 21 (2020) 1–9. <https://doi.org/10.1016/j.cogsc.2019.11.001>
- [5] Biochar as eco-friendly conductive material for terahertz applications, *Sci. Rep.* 11 (2021) 19156. <https://doi.org/10.1038/s41598-021-98009-5>
- [6] P.T. Le, H.T. Bui, D.N. Le, et al., Preparation and characterization of biochar from agricultural waste, *J. Chem.* (2021) 9161904. <https://doi.org/10.1155/2021/9161904>
- [7] A.C. Ferrari, J. Robertson, Interpretation of Raman spectra of disordered and amorphous carbon, *Phys. Rev. B* 61 (2000) 14095–14107. <https://doi.org/10.1103/PhysRevB.61.14095>
- [8] A.C. Ferrari, D.M. Basko, Raman spectroscopy as a tool for graphene, *Nat. Nanotechnol.* 8 (2013) 235–246. <https://doi.org/10.1038/nnano.2013.46>
- [9] J. Robertson, Diamond-like amorphous carbon, *Mater. Sci. Eng. R* 37 (2002) 129–281. [https://doi.org/10.1016/S0927-796X\(02\)00005-0](https://doi.org/10.1016/S0927-796X(02)00005-0)
- [10] S. Iijima, Helical microtubules of graphitic carbon, *Nature* 354 (1991) 56–58. <https://doi.org/10.1038/354056a0>
- [11] F. Kremer, A. Schönhals, *Broadband Dielectric Spectroscopy*, Springer, 2003. <https://doi.org/10.1007/978-3-642-56120-7>
- [12] H. Sirringhaus, Device physics of solution-processed organic field-effect transistors, *Adv. Mater.* 17 (2005) 2411–2425. <https://doi.org/10.1002/adma.200501152>
- [13] M. Dressel, G. Grüner, *Electrodynamics of Solids*, Cambridge University Press, 2002. <https://doi.org/10.1017/CBO9780511606168>
- [14] Y. Li, et al., Flexible dielectric materials for organic electronics, *Adv. Funct. Mater.* 28 (2018) 1805516. <https://doi.org/10.1002/adfm.201805516>
- [15] J. Lehmann, S. Joseph, *Biochar for environmental management*, Earthscan, 2015.
- [16] D. Mohan, A. Sarswat, Y.S. Ok, C.U. Pittman Jr., Organic contaminant removal using biochar, *Bioresour. Technol.* 160 (2014) 191–202. <https://doi.org/10.1016/j.biortech.2014.01.120>
- [17] A. Downie, A. Crosky, P. Munroe, Physical properties of biochar, *Biochar Environ. Manag.* (2012) 13–32.
- [18] X. Zhang, et al., Biochar-based composite materials for energy storage, *J. Energy Storage* 25 (2019) 100841. <https://doi.org/10.1016/j.est.2019.100841>
- [19] J. Wang, S. Kaskel, KOH activation of carbon-based materials for energy storage, *J. Mater. Chem.* 22 (2012) 23710–23725. <https://doi.org/10.1039/C2JM34066F>
- [20] Y. Sun, B. Gao, Y. Yao, et al., Effects of feedstock and pyrolysis temperature on biochar properties, *Bioresour. Technol.* 102 (2011) 3488–3497. <https://doi.org/10.1016/j.biortech.2010.10.081>